

# Explore New Cellular Frontiers



## See More. Sort More.

Welcome to a new reality where high-complexity assays optimized on the Cytex® Aurora can now be run on the Aurora CS for sorting.

As a sorter, the CS offers the flexibility required to meet various biological and sorting conditions, including 6-way sorting, customizable sort modes, automated drop delay and stream monitoring. This is combined with all the benefits of full spectrum profiling (FSP™) technology.

The result is a system that delivers high resolution at the single cell level to resolve and isolate the most challenging cell populations, such as cells with high autofluorescence or low-level expression of key biomarkers, regardless of assay complexity.

## Solve More Biological Questions

Cytex's total cell analysis solutions put the power of discovery in your hands. From immunology and oncology to infectious disease, drug discovery, and more – Cytex empowers researchers like you to answer the toughest biological questions.

### A Seamless Cell Sorting Experience Awaits You with the New Aurora CS

Let's Get Sorting




[https://welcome.cytexbio.com/takefocus\\_immuno](https://welcome.cytexbio.com/takefocus_immuno)

# The cytosolic tryparedoxin peroxidase from *Trypanosoma cruzi* induces a pro-inflammatory Th1 immune response in a peroxidatic cysteine-dependent manner

Lucía López,<sup>1,2</sup>


María Laura Chiribao,<sup>2,3</sup>

Magali C. Girard,<sup>4</sup>

Karina A. Gómez,<sup>4</sup> 

Paula Carasi,<sup>1</sup> Marisa Fernandez,<sup>5</sup>

Yolanda Hernandez,<sup>5</sup>

Carlos Robello,<sup>2,3</sup> Teresa Freire<sup>1</sup> 

and María Dolores Piñeyro<sup>2,3</sup>

<sup>1</sup>Laboratorio de Inmunomodulación y Desarrollo de Vacunas, Departamento de Inmunobiología, Facultad de Medicina, Universidad de La República, Montevideo, Uruguay, <sup>2</sup>Unidad de Biología Molecular, Institut Pasteur Montevideo, Montevideo, Uruguay, <sup>3</sup>Departamento de Bioquímica, Facultad de Medicina, Universidad de La República, Montevideo, Uruguay, <sup>4</sup>Laboratorio de Inmunología de las Infecciones por Tripanosomátidos, Instituto de Investigaciones en Ingeniería Genética y Biología Molecular (INGEBI-CONICET), Buenos Aires, Argentina and <sup>5</sup>Instituto Nacional de Parasitología 'Doctor Mario Fatala Chabén', Buenos Aires, Argentina

doi:10.1111/imm.13302

Received 17 September 2020; revised 25 November 2020; accepted 19 December 2020.

Teresa Freire and María Dolores Piñeyro contributed equally to this work.

## Correspondence

Teresa Freire, Facultad de Medicina, Departamento de Inmunobiología, UdelaR, Montevideo, Uruguay.

Email: tfreire@fmed.edu.uy

María Dolores Piñeyro, Facultad de Medicina, Departamento de Bioquímica, Udelar, Montevideo, Uruguay.

Email: mpineyro@fmed.edu.uy

Senior author: Teresa Freire, tfreire@fmed.edu.uy

\*Both authors contributed equally to this work

## Summary

*Trypanosoma cruzi* cytosolic tryparedoxin peroxidase (c-TXNPx) is a 2-Cys peroxiredoxin (Prx) with an important role in detoxifying host cell oxidative molecules during parasite infection. c-TXNPx is a virulence factor, as its overexpression enhances parasite infectivity and resistance to exogenous oxidation. As Prxs from other organisms possess immunomodulatory properties, we studied the effects of c-TXNPx in the immune response and analysed whether the presence of the peroxidatic cysteine is necessary to mediate these properties. To this end, we used a recombinant c-TXNPx and a mutant version (c-TXNPxC52S) lacking the peroxidatic cysteine. We first analysed the oligomerization profile, oxidation state and peroxidase activity of both proteins by gel filtration, Western blot and enzymatic assay, respectively. To investigate their immunological properties, we analysed the phenotype and functional activity of macrophage and dendritic cells and the T-cell response by flow cytometry after injection into mice. Our results show that c-TXNPx, but not c-TXNPxC52S, induces the recruitment of IL-12/23p40-producing innate antigen-presenting cells and promotes a strong specific Th1 immune response. Finally, we studied the cellular and humoral immune response developed in the context of parasite natural infection and found that only wild-type c-TXNPx induces proliferation and high levels of IFN- $\gamma$  secretion in PBMC from chronic patients without demonstrable cardiac manifestations. In conclusion, we demonstrate that c-TXNPx possesses pro-inflammatory properties that depend on the presence of peroxidatic cysteine that is essential for peroxidase activity and quaternary structure of the protein and could contribute to rational design of immune-based strategies against Chagas disease.

**Keywords:** immune response; peroxiredoxin; *Trypanosoma cruzi*.

Abbreviations: C<sub>p</sub>, peroxidatic cysteine; Prx, peroxiredoxin; TXNPx, tryparedoxin peroxidase

## Introduction

*Trypanosoma cruzi*, a protozoan parasite, is the causative agent of Chagas disease, a potentially life-threatening illness and a major public healthcare problem in the Americas. Six to seven million people worldwide are estimated to be infected with *T. cruzi*, with 28 million living in endemic areas, causing around 14 000 deaths annually.<sup>1</sup> There has been an expansion of the disease in the past decades due to migration, and it has been increasingly detected in Canada, and many European and some Western Pacific countries.<sup>2</sup> No vaccines are available, and current trypanocidal treatment causes frequent adverse events.<sup>3,4</sup>

Once *T. cruzi* infects a mammal, it invades different cell types including macrophages, muscle cells (smooth and striated) and fibroblasts. Macrophages are one of the first cell line of defence of the innate immune response in vertebrates that play a central role in the control of *T. cruzi* infection, but their deactivation favours parasite evasion.<sup>5,6</sup> Indeed, *T. cruzi* is able to cope with the oxidative environments found in the hosts and ensure infection due to an efficient antioxidant system, based on trypanothione metabolism, a dithiol unique from kinetoplastids. As part of this trypanothione-dependent system, trypanothione peroxidases, one cytosolic (c-TXNPx) and one mitochondrial (m-TXNPx), catalyse the reduction of a broad spectrum of substrates including hydrogen peroxide (H<sub>2</sub>O<sub>2</sub>), peroxynitrite (ONOO<sup>-</sup>) and organic hydroperoxides (ROOH).<sup>7</sup> The *T. cruzi* TXNPx enzymes are typical 2-Cys peroxiredoxins (Prxs), which possess two conserved cysteine residues essential for their catalytic activity. The peroxidatic cysteine (C<sub>P</sub>) is responsible for the reduction of the peroxide substrate, while the resolving cysteine (C<sub>R</sub>) is involved in the formation of the intermolecular disulphide bond during the catalytic cycle.<sup>8</sup> In general, active Prxs exist as homodecamers organized as a pentamer of dimers.<sup>8</sup>

Several lines of evidence indicate that Prxs may constitute key enzymes in trypanosomatids as they play relevant roles in *T. cruzi* infection process, constituting virulence factors. Overexpression of c-TXNPx is associated with an increase in parasite infectivity in both phagocytic and non-phagocytic cells<sup>9</sup> and with an increased resistance to exogenous H<sub>2</sub>O<sub>2</sub> and ONOO<sup>-</sup>.<sup>10</sup> Consistent with these findings, virulent strains express higher levels of c-TXNPx as compared to attenuated parasitic isolates.<sup>11</sup>

Interestingly, the functions of Prxs go far beyond their antioxidant activity. Indeed, they can also present chaperone activity that protects protein substrates from stress-induced aggregation.<sup>12</sup> This new function is linked to the inactivation of Prxs by overoxidation of the active cysteine, which involves the reaction of sulphenic (-SOH) acid with another molecule of H<sub>2</sub>O<sub>2</sub> generating sulphinic

(-SO<sub>2</sub>H) or sulphonic (-SO<sub>3</sub>H) acid at the active 2-Cys Prx C<sub>P</sub>.<sup>13</sup> Prxs show different susceptibilities to overoxidation depending on the presence of two structural elements: a Gly-Gly-Leu-Gly motif and the presence of a Tyr-Phe sequence in the C-terminal arm.<sup>14</sup> In particular, *T. cruzi* c-TXNPx is overoxidized in oxidative stress conditions and has chaperone activity.<sup>15</sup>

Prxs can also modulate inflammation, immunity and tissue repairing reactions.<sup>16,17</sup> Different studies have demonstrated the secretion and immunomodulatory properties of Prxs. The secretion of Prxs from humans<sup>18,19</sup> or helminth parasites<sup>20</sup> has been demonstrated. In kinetoplastids, TXNPx has been detected in the secretome of different organisms, such as *T. cruzi*, *T. brucei* and *Leishmania donovani*.<sup>21–24</sup>

With respect to their immunomodulatory properties, the Prx from the protozoa *Plasmodium berghei*, the causative agent of malaria in rodents, induces the secretion of TNF- $\alpha$  and shifts T-cell response towards an inflammatory Th1 profile,<sup>25</sup> while the helminth *Fasciola hepatica* Prx drives T-cell polarization towards a Th2 phenotype.<sup>26</sup> Furthermore, Prxs can favour parasite survival by modulating the host immune response.<sup>27–29</sup> In fact, the Prx from *Toxoplasma gondii* modulates the function of macrophages by inhibiting the production of IL-1 $\beta$  and increasing IL-10 secretion.<sup>28</sup> In a previous work, we demonstrated that in the context of natural infection, c-TXNPx induces proliferation but not IFN- $\gamma$  secretion from peripheral blood mononuclear cells (PBMC) of patients with chronic Chagas disease without any clinical symptoms, but not in those with cardiac alterations.<sup>30</sup> In view of these results, we speculate that the weak immune response triggered by c-TXNPx could be an evasion strategy developed by *T. cruzi* due to parasite-host coevolution.

Following this line of research, the aim of this work was to study the effects of c-TXNPx in the innate and adaptive immune response in a murine experimental model and analyse whether its C<sub>P</sub> is necessary to mediate these immunological properties. To this purpose, we produced recombinant forms of wild-type (wt) active c-TXNPx and a mutant in the C<sub>P</sub> by replacing cysteine 52 with serine (c-TXNPxC52S). Our results show that only c-TXNPx, but not c-TXNPxC52S, induced the recruitment of IL-12/23p40-producing innate antigen-presenting cells (APCs) associated with a strong specific Th1 immune response that depends on the presence of the redox active cysteine. These effects can be attributed to the presence of the C<sub>P</sub> and eventually to a change in the quaternary conformation of the protein as both proteins differ in their oligomerization state. In accordance with data obtained in mice immunized with c-TXNPx or the inactive protein, only c-TXNPx provoked proliferation and an increase of IFN- $\gamma$  levels in chronic patients, but this response was only higher in those patients without

cardiac manifestations when compared among the groups.

## Materials and methods

### Recombinant c-TXNPx and c-TXNPxC52S expression and purification

The cytosolic trypanothione peroxidase wt and C<sub>P</sub> mutants (c-TXNPx and c-TXNPxC52S) were expressed and purified as previously described with modifications.<sup>31</sup> Clear-Coli BL21 (DE3) bacterial strain, expressing a human non-endotoxic form of lipopolysaccharide (LPS),<sup>32</sup> was used. Plasmid pQE30-*TcH6TXNPx* or pQE30-*TcH6TXNPxC52S* in the selected bacteria was grown at 30°C in LB–Miller medium. Mock control was produced from the extract of bacteria transformed with the same vector used for recombinant c-TXNPx production (without the gene) submitted to the same purification process. Residual endotoxins were removed from protein sample using the Thermo Scientific Pierce High Capacity Endotoxin Removal Resin (Thermo Scientific Pierce, MA, USA) and measured by commercial Kit LAL Pyrochrome (Associates of Cape Cod, Incorporated) obtaining 0.637 UE/μg protein for c-TXNPx and 0.0165 UE/μg protein for c-TXNPxC52S, which are in accordance with the amount of endotoxin allowed for inoculation in mice.<sup>33</sup> Endotoxins were also measured by the capacity of the proteins to trigger TLR4 signalling. To this end, TLR4-expressing 293HEK cells (Invivogen), kindly provided by Dr. Eduardo Osinaga, were incubated with the recombinant proteins overnight at 37°C, and IL-8 production was evaluated by specific sandwich ELISA.

### Peroxidase activity assay

Peroxidase activity of c-TXNPx and c-TXNPxC52S was measured by monitoring NADPH consumption at 340 nm using the coupled assay to regenerate the c-TXNPx in its reduced form. All enzyme assays were performed on 384-well plates (Nunc, Denmark) in a final volume of 50 μl at 25°C using a Multiskan Ascent one-channel vertical light-path filter photometer (Thermo Electron Co.). The reaction mixture contained the following: 50 mM buffer HEPES buffer, pH 7.4, 1 mM EDTA, 300 μM NADPH, 2 μM *T. cruzi* trypanothione reductase (TR), 5 μM *T. cruzi* trypanothione 1 (TXN1), 50 μM trypanothione (TSH<sub>2</sub>), and c-TXNPx wt or C<sub>P</sub> mutant (5 μM). For TR and TXN1 purification, expression plasmids were gently provided by Diego Arias, and TSH<sub>2</sub> was gently provided by Marcelo Comini. Reactions were started by the addition of 40 to 200 μM H<sub>2</sub>O<sub>2</sub>. Kinetic data were plotted as initial velocity or *v*<sub>0</sub> (μM min<sup>-1</sup>) versus substrate concentration (μM). Three independent sets of data were generated. Results are

expressed as specific activity (U/mg), calculated in the following manner:

Initial velocity was calculated as μM NADPH/min using the molar extinction coefficient of NADPH ( $\epsilon = 6220 \mu\text{M}^{-1}\text{cm}^{-1}$ ) and the optical path (0.5 cm) using Equation (1):

$$v_0(\text{NADPH}/\text{min}) = v_0 \div (\epsilon \times \lambda) \quad (1)$$

Enzymatic activity (*U*) was calculated using Equation (2).

$$U(\mu\text{MNADPH}/\text{min}) = v_0 \times \text{Volreaction}(\text{ml}) \quad (2)$$

Specific enzymatic activity (*U*<sub>esp</sub>) was calculated using Equation (3).

$$U_{\text{esp}}(\text{U}/\text{mg}) = (U \times \text{proteinconcentration})\%(\text{volprotein}(\text{ml})) \quad (3)$$

### Overoxidation state of c-TXNPx by Western blot

Purified recombinant c-TXNPx treated for endotoxin removal was assayed to determine the overoxidation state was done as in Ref. 15. Briefly, recombinant c-TXNPx was assayed for the presence of a sulphonic or sulphinic acid in the C<sub>P</sub> by Western blot using an anti-peroxiredoxin–SO<sub>3</sub> (anti-Prx-SO<sub>3</sub>), which recognizes the sulphonylated peptide corresponding to the conserved active site sequence of Prxs. An overoxidized c-TXNPx was used as a positive control.

### Gel filtration chromatography

Gel filtration chromatography was performed at 25°C by AKTA pureTM system (GE Healthcare) on a Superdex 200 column 10/300 (Pharmacia). The column was equilibrated with 50 mM sodium phosphate (pH 7.4) and 100 mM NaCl at a flow rate of 1 ml/min. The sample volume for each run was 500 μl at a concentration of 1 mg/ml. Absorbance at 280 nm was measured to monitor protein elution profiles. Thyroglobulin (669 kDa), ferritin (440 kDa), aldolase (158 kDa), conalbumin (75 kDa), ovalbumin (44 kDa) and lysozyme (14.7 kDa) were used as molecular mass standards (GE Healthcare Calibration Kit).

### Ethics statement

Mouse experiments were carried out in accordance with strict guidelines from the National Committee on Animal Research (Comisión Nacional de Experimentación Animal, CNEA, National Law 18.611, Uruguay). All procedures involving animals were approved by the Universidad de la República's Committee on Animal Research (Comisión Honoraria de Experimentación Animal, CHEA Protocol Numbers: 070153-000320-13).



The research protocol with patients or non-infected individuals was approved by the Bioethics Committee of National Institute of Parasitology 'Dr. Mario Fatała Chabén' (INH:FWA: 00017212), Buenos Aires, Argentina. All enrolled subjects gave written informed consent in compliance with the guidelines of the Ethical Committee of the Institute.

### Mice

Six- to 10-week-old female BALB/c mice were obtained from DiLaVe Laboratories or Institut Pasteur de Montevideo (Uruguay). Animals were kept in the animal house (URBE, Facultad de Medicina, UdelaR, Uruguay) with water and food supplied *ad libitum*. Either c-TXNPx or c-TXNPxC52S was injected i.p. in BALB/c mice three times a week for 2 weeks (20 µg/mouse) in PBS, as previously reported.<sup>26,27</sup> As control, a similar volume of a mock preparation was also injected in PBS. Two days after the last injection, mice were killed and bled, and spleens and peritoneal exudate cells (PEC) were collected.

### Study population

The study population was recruited at the National Institute of Parasitology 'Dr. Mario Fatała Chabén', Buenos Aires, Argentina. *T. cruzi* infection was determined by indirect immunofluorescence, enzyme-linked immunosorbent assay (ELISA) and/or indirect haemagglutination (IHAs). Subjects who had at least two of three tests positive were considered to be infected. Patients, in the chronic phase of the infection, underwent a complete clinical and cardiological examination and were stratified as patients without demonstrable cardiac involvement (Group 0, G0) or patients with Chagas cardiomyopathy (Group 1, G1).<sup>34</sup> Eleven adult volunteers showing negative serological tests for Chagas' disease were included as non-infected individuals (NI, control group). All groups of individuals were matched for age and gender (Table 1). The exclusion criteria included no record of treatment with benznidazole or nifurtimox, the presence of systemic arterial hypertension, diabetes mellitus, thyroid dysfunction, renal insufficiency, chronic obstructive pulmonary disease, hydroelectrolytic disorders, alcoholism and history suggesting coronary artery obstruction and rheumatic disease, and the impossibility of undergoing the examinations. PBMCs were isolated by Ficoll-Hypaque density gradient centrifugation (GE Healthcare BioSciences AB, Uppsala, Sweden), within 4 h after blood collection in EDTA-anticoagulated tubes. Isolated PBMCs were resuspended in fetal bovine serum (FBS; Natocor, Córdoba, Argentina) containing 10% dimethyl sulphoxide (DMSO), and cryopreserved in liquid N<sub>2</sub> until used. An aliquot of whole blood 4 ml from each subject was

Table 1. Characteristics of patients and controls included in this work

	Patients with chronic Chagas disease		
	Without cardiac involvement (G0)	With cardiac involvement (G1)	Non- <i>T. cruzi</i> -infected individuals (NI)
Number of individuals ( <i>n</i> )	10	14	11
Gender (female/male)	5-5	6-8	7-4
Age (media and range)	60 (57–70)	55 (42–67)	43 (29–57)
Kuschnir stages (0-1-2-3)	0-0-0-0	0-12-1-1	NA
Range of anti- <i>T. cruzi</i> antibody titre <sup>a</sup>	4629 - 99407	1000 - 30318	NA

NA, not applicable.

<sup>a</sup>The titre of anti-*T. cruzi* antibodies was considered as IC<sub>50</sub> serum dilution factor. Patients were stratified according to the modified Kuschnir classification.<sup>26</sup>

separated and centrifuged at 400 g to obtain the sera, which was stored at -20° until use.

### Analyses of mouse PECs and splenocytes by flow cytometry

PECs from mice were washed twice with PBS containing 2% FBS and 0.1% sodium azide (wash buffer) and incubated with the following antibodies: anti-CD11c (N418), anti-I-A/I-E (2G9), anti-CD40 (HM40-3), anti-F4/80 (BM8), anti-CD11b (M1/70), anti-Ly6C (HK1.4) and anti-Ly6G (RB6-8C5). Cells were then washed twice with wash buffer and fixed with 0.1% formaldehyde. Cell populations were analysed using a BD Accuri (BD Biosciences) or Cyan (Beckman Coulter). Expression of IL-10 and IL-12/23p40 was analysed by intracellular staining. Antibodies were obtained from Affymetrix (CA, USA), BD Biosciences (CA, USA) or Biologend (CA, USA).

### Analyses of splenocyte proliferation

Mouse CFSE-labelled splenocytes (1 × 10<sup>6</sup> cell/well) were incubated in the presence of either c-TXNPx, c-TXNPxC52S (20 µg/ml) or mock diluted in complete culture medium consisting of RPMI-1640 with glutamine (PAA Laboratories, Austria) supplemented with 10% heat-inactivated FBS, 50 µM 2-mercaptoethanol, 100 U/ml penicillin and 100 mg/ml streptomycin (Sigma-

Aldrich, St. Louis, MO) for 5 days at 37° in 5% CO<sub>2</sub>. Then, cells were stained with anti-CD4 or anti-CD8 antibodies and analysed by flow cytometry. The proliferation index was calculated as the ratio between the percentages of CFSE<sup>low</sup> cells in treated and control cells with respect to the control (medium alone). IL-4 and IFN- $\gamma$  on the culture supernatants were quantified by interleukin-specific sandwich ELISAs (BD Bioscience, NJ, USA) according to the manufacturer's instructions.

### Antibody titres

IgM, IgG and IgG2a antibody titres in sera from immunized mice were evaluated by ELISA. Briefly, 96-well microtitre plates (Nunc, Denmark) were coated overnight at 4° with 1–2  $\mu$ g/well of c-TXNPx or c-TXNPx52S in 50 mM carbonate buffer (pH 9.6). After blocking with 1% gelatine in PBS, three washes with PBS containing 0.1% Tween-20 were performed. Serially diluted sera in buffer (PBS containing 0.1% Tween-20 and 0.5% gelatine) were added to the wells for 1 h at 37°C. Following three washes, wells were treated for 1 h at 37° using goat anti-mouse IgM, IgG or IgG2a peroxidase conjugates or rabbit anti-human IgG peroxidase conjugate (Sigma-Aldrich, St. Louis, MO) and *o*-phenylenediamine (OPD) or tetramethylbenzidine (TMB) and H<sub>2</sub>O<sub>2</sub> were then added as substrate. Plates were read photometrically at 492 nm in an ELISA autoreader (LabSystems Multiskan MS, Finland). Antibody titres were calculated to be the log<sub>10</sub> highest dilution, which gave twice the absorbance of control (mock) mouse sera with the minor dilution. Titres are shown as the arithmetic mean  $\pm$  SEM of the log<sub>10</sub> titres.

Alternatively, antibody titre from each patient or non-infected donors was determined by ELISA, as previously described.<sup>30</sup> Data were shown as the serum dilution factor that corresponds to 50% of the maximum response (IC50) calculated by non-linear, dose–response regression analysis using the GraphPad Prism software.<sup>30</sup>

### Human PBMC stimulation and culture

PBMCs ( $2 \times 10^5$  cells/well) were stimulated in triplicates with recombinant c-TXNPx or c-TXNPx52S (10  $\mu$ g/ml) or no antigen (culture medium alone) in 200  $\mu$ l of RPMI medium containing 100 U/ml penicillin, 100  $\mu$ g/ml streptomycin, 2 mM L-glutamine and 5% heat-inactivated male AB Rh-positive human serum (HS; Sigma, St Louis, MO, USA). 'Mock' stimulations were included to control the background response potentially induced by contaminants from the recombinant protein production process. Non-specific stimulation with 1  $\mu$ g/ml phytohaemagglutinin (PHA, Sigma, St Louis, MO, USA) and specific stimulation with whole *T. cruzi* epimastigote lysate (10  $\mu$ g/ml) were used as positive control conditions (data

not shown). After 5 days of incubation, culture supernatants were collected and stored at –20° until IFN- $\gamma$  secretion assessment. Subtracted medium was replaced with complete RPMI medium, and cells were pulsed for 18 h with 0.5  $\mu$ Ci/well [methyl-<sup>3</sup>H]-thymidine (PerkinElmer, Waltham, MA, USA) after which they were harvested on glass fibre filters. Proliferation was measured as incorporated radioactivity, assessed by liquid scintillation counting. INF- $\gamma$  secretion was measured by ELISA (OptEIA™ Human IFN- $\gamma$  ELISA set, BD Pharmingen, San Diego, CA, USA) according to the manufacturer's instructions.

### Statistical analysis

Results were analysed using the GraphPad Prism software (GraphPad Software, San Diego, CA) with one-way ANOVA with the Bonferroni multiple comparison test or Student's *t* test. For human experiments, we first analysed the normality and homoscedasticity of the data using the Shapiro–Wilk normality test and Bartlett test, respectively. Data from proliferation and IFN- $\gamma$  secretion were transformed by log<sub>10</sub> to obtain a Gaussian distribution of errors and homoscedasticity. Linear mixed-effects models (LMMs) fitted by maximum likelihood and Tukey's honest significant difference (HSD) contrasts for post hoc comparisons were applied to analyse data. LMM was performed using groups G0, G1, NI and stimulation condition as fixed factors and patient as a random factor. LMMs were fitted in R3.2.1 (Team RC 2013), using the function lmer of the R package lme4 (Bates DM 2010). Tukey's HSD contrasts with adjusted *p* values (Bonferroni) were applied as post hoc comparisons, using the ght function of the R package multcomp.<sup>35</sup> In all cases, a *P* value of less than 0.05 (\*) or 0.01 (\*\*) was considered statistically significant.

## Results

### Biochemical characterization of c-TXNPx and c-TXNPx52S

A recombinant wt c-TXNPx and mutant in C<sub>p</sub> c-TXNPx52S (Figure 1A) from *T. cruzi* were produced in ClearColi BL21 (DE3) strain, purified by affinity chromatography followed by incubation with a polymyxin B column to remove residual endotoxins. We also generated a control termed mock from bacteria transformed with the empty vector and subjected to the same procedures than both recombinant proteins. First, in order to guarantee that c-TXNPx is in its reduced and active form, we performed a coupled assay that measures the decay in NADPH absorbance in the presence of all components of the regenerating system.<sup>15</sup> As shown in Figure 1B,C, endotoxin removal did

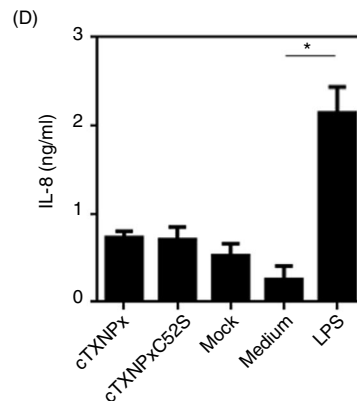
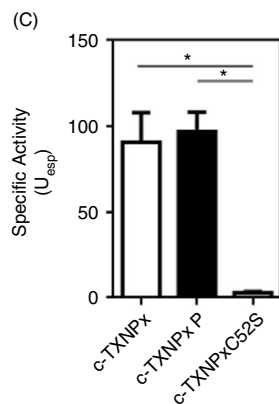
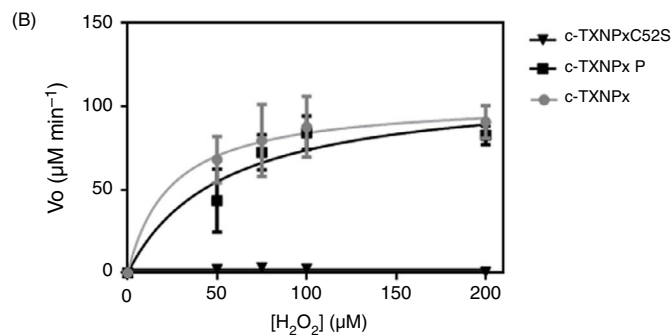
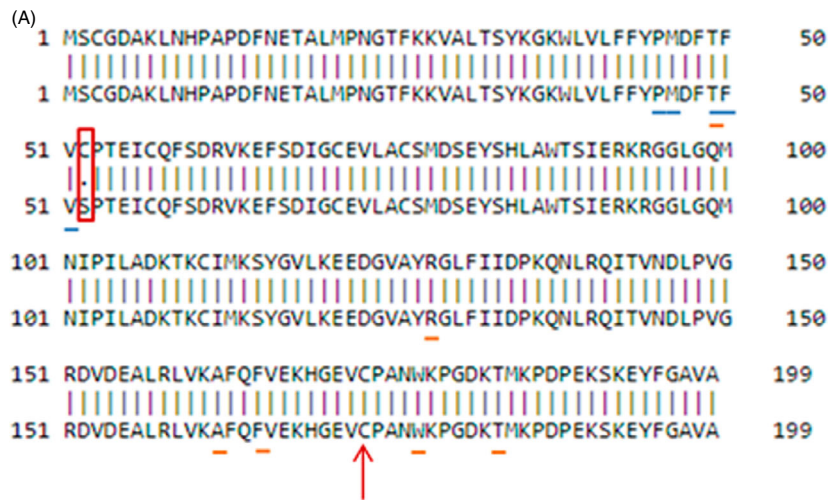


**Figure 1.** Peroxidase activity of c-TXNPx and mutant c-TXNPxC52S. (A) Protein sequence alignment of c-TXNPx and c-TXNPxC52S. 'Pairwise Sequence Alignment' software was used. Cp is denoted by a red box; Cr by a red arrow. Amino acids in the active site are marked in blue, and residues involved in activity are shown in orange. (B) Kinetics of H<sub>2</sub>O<sub>2</sub> reduction by wild-type c-TXNPx and mutant version (5 μM) were measured by a coupled assay. Kinetic parameters were determined by monitoring NADPH consumption at 340 nm. Reactions were carried out in the presence of 300 μM NADPH, 2 μM *T. cruzi* trypanothione reductase, 5 μM of *T. cruzi* trypanothione, 5 μM of *T. cruzi* trypanothione reductase, 5 μM of *T. cruzi* trypanothione, 5 μM of trypanothione, and 40 to 200 μM of H<sub>2</sub>O<sub>2</sub>, at pH 7.4 and 25°. Wild-type and mutant c-TXNPx expressed in ClearColi DB3 strain (c-TXNPx, c-TXNPxC52S) and c-TXNPx after the endotoxin removal with Polymyxin B (c-TXNPx P). (C) Specific activity (U/mg) of c-TXNPx, c-TXNPx P and c-TXNPxC52S was calculated as explained in Materials and Methods. Data are representative of three independent experiments. (D) Determination of TLR4 signalling by TXNPx P and c-TXNPxC52S P. 293HEK cells overexpressing murine TLR4 were incubated overnight at 37°C with 30 μg/ml of each protein. Human IL-8 was detected on culture supernatants by specific sandwich ELISA.

not alter peroxidase activity of purified c-TXNPx at all H<sub>2</sub>O<sub>2</sub> concentrations assayed. On the other hand, the mutant in Cp, c-TXNPxC52S, had no peroxidase

activity.<sup>31</sup> Importantly, both recombinant proteins did not show any differences with the mock control in their capacity to stimulate TLR4 signalling in TLR4-

expressing 293HEK cells (Figure 1D), indicating that they present similar low endotoxin levels.

The majority of wt c-TXNPx treated for endotoxin removal was not overoxidized, when compared to the overoxidized c-TXNPx (Figure S1). Considering that overoxidation of sulphenic (-SOH) acid to sulphinic (-SO<sub>2</sub>H) or sulphonic (-SO<sub>3</sub>H) acid of the 2-Cys Prx C<sub>p</sub> causes inactivation of peroxidase activity of TXNPx and an increase in chaperone activity,<sup>13,15</sup> our data confirm that wt c-TXNPx used in the immunological assay retained peroxidase activity, when it can be regenerated.

Prior studies have shown that Prx overoxidation due to oxidative stress or heat shock favours the formation of high molecular weight complexes and this structural shift from low molecular mass oligomers to high molecular mass (HMM) aggregates accompanies a functional change in these enzymes from peroxidase to chaperone activity.<sup>36,37</sup> We have previously demonstrated that wt c-TXNPx and mutant c-TXNPxC52S have different structural profiles under different redox conditions.<sup>15</sup> Before the immunological assays, the wt c-TXNPx and C<sub>p</sub> mutant c-TXNPxC52S proteins expressed in another bacterial strain, endotoxin-free (*ClearColi*) and without any redox treatment, were tested for structural profiles by gel filtration showing a similar profile as the non-endotoxin-free proteins (Figure S1B). Both proteins eluted in two forms: c-TXNPx eluted in two peaks of 690 and 350 kDa, which corresponded to HMM aggregates; and an oligomer composed of 14 monomers, respectively. Mutant c-TXNPxC52S also eluted as two major peaks, one broad of 570–1300 kDa and another corresponding to the MW of a decamer (250 kDa). These results show that after purification and endotoxin removal, wt c-TXNP and C<sub>p</sub> mutant were present as a mixture of two species, indicating that C<sub>p</sub> is not necessary for the formation of decameric form and higher mass aggregate structures of the protein. It also implies that wt c-TXNPx and C<sub>p</sub> mutant have different macromolecular structures, which could render a different antigen processing.

#### wt c-TXNPx recruits IL-12/23p40-producing innate APC and induces a specific Th1 immune response

In order to analyse the effect of c-TXNPx on innate APCs and to determine whether it depends on the wt c-TXNPx, which has the redox active C<sub>p</sub>, we injected mice with c-TXNPx or its inactive c-TXNPxC52S mutant in the peritoneal cavity and analysed the presence of CD11c<sup>+</sup> F4/80<sup>-</sup> and F4/80<sup>+</sup> CD11c<sup>-</sup> cells, their phenotype and cytokine production capacity (Figure S2). Macrophages and dendritic cells belong to the mononuclear phagocytic system; F4/80 is a common marker for murine macrophages, while CD11c is used to identify murine dendritic cells.<sup>38</sup> Although mice injected with c-TXNPx and c-TXNPxC52S presented similar frequency of CD11c<sup>+</sup> in the peritoneal

cavity, they were higher with respect to the control group (mock) (Figure 2A). Furthermore, increased levels of F4/80<sup>+</sup> cells were detected in both groups (Figure 2B), although the mutated protein induced a twofold increase in F4/80<sup>+</sup> cells as compared to the wt protein.

In addition, peritoneal CD11c<sup>+</sup> cells were characterized by a low expression of the granulocyte or macrophage markers Ly6G and CD68, low (for c-TXNPx) or intermediate (for c-TXNPxC52S) levels of the monocyte marker Ly6C, and high levels of MHC class II (Figure 2C) in relation to cells from mock-treated mice. However, peritoneal F4/80<sup>+</sup> cells presented a different phenotype in mice injected with c-TXNPx or c-TXNPxC52S. While in both cases, F4/80<sup>+</sup> cells expressed similar levels of MHC class II and the macrophage marker CD68, F4/80<sup>+</sup> cells from c-TXNPxC52S-injected mice expressed increased levels of Ly6G and Ly6C with regard to those from c-TXNPx-injected mice (Figure 2D).

Last, only CD11c<sup>+</sup> or F4/80<sup>+</sup> cells from mice injected with the wt c-TXNPx significantly increased IL-12/23p40 production, but not IL-10, as compared to the control group (Figure 2E,F). These results suggest that both proteins were capable of inducing a recruitment of innate APCs in the site of injection, although in the absence of redox active C<sub>p</sub>, these cells display a granulocytic/macrophage phenotype and a more pronounced recruitment of these cells was favoured. However, only the wt enzyme stimulated the significant production of IL-12/23p40 from both CD11c<sup>+</sup> and F4/80<sup>+</sup> cells, suggesting that the presence of C<sub>p</sub> is needed to induce a pro-inflammatory phenotype in these cells, possibly due to the conformational structure of the wt protein.

To analyse whether there was an association between alterations in the phenotype of peritoneal innate APCs with the adaptive immune response, we next analysed the T-cell response induced by c-TXNPx and c-TXNPxC52S. When splenocytes from c-TXNPx- or c-TXNPxC52S-injected mice were *in vitro*-stimulated with the corresponding proteins, we observed a higher proliferation index for CD4<sup>+</sup> and CD8<sup>+</sup> T cells together with higher IFN- $\gamma$ , but not IL-4 secretion levels by splenocytes from animals injected with c-TXNPx than c-TXNPxC52S or mock (Figure 3A). These results might indicate that the inactive protein induces an impaired T-cell response, while the wt c-TXNPx prompts a stronger specific Th1 immune response.

We next analysed in depth the specificity of the T-cell immune response induced by both c-TXNPxs and whether the replacement of C<sub>p</sub> affected T-cell proliferation. To this end, we carried out experiments to evaluate the cross-reactivity of CD4<sup>+</sup> or CD8<sup>+</sup> T cells for c-TXNPx and c-TXNPxC52S. CD4<sup>+</sup>, but not CD8<sup>+</sup> T cells, from mice *in vivo primed* with the wt protein and restimulated *in vitro* with the mutated c-TXNPx (c-TXNPx/c-TXNPxC52S) exhibited higher proliferation index than



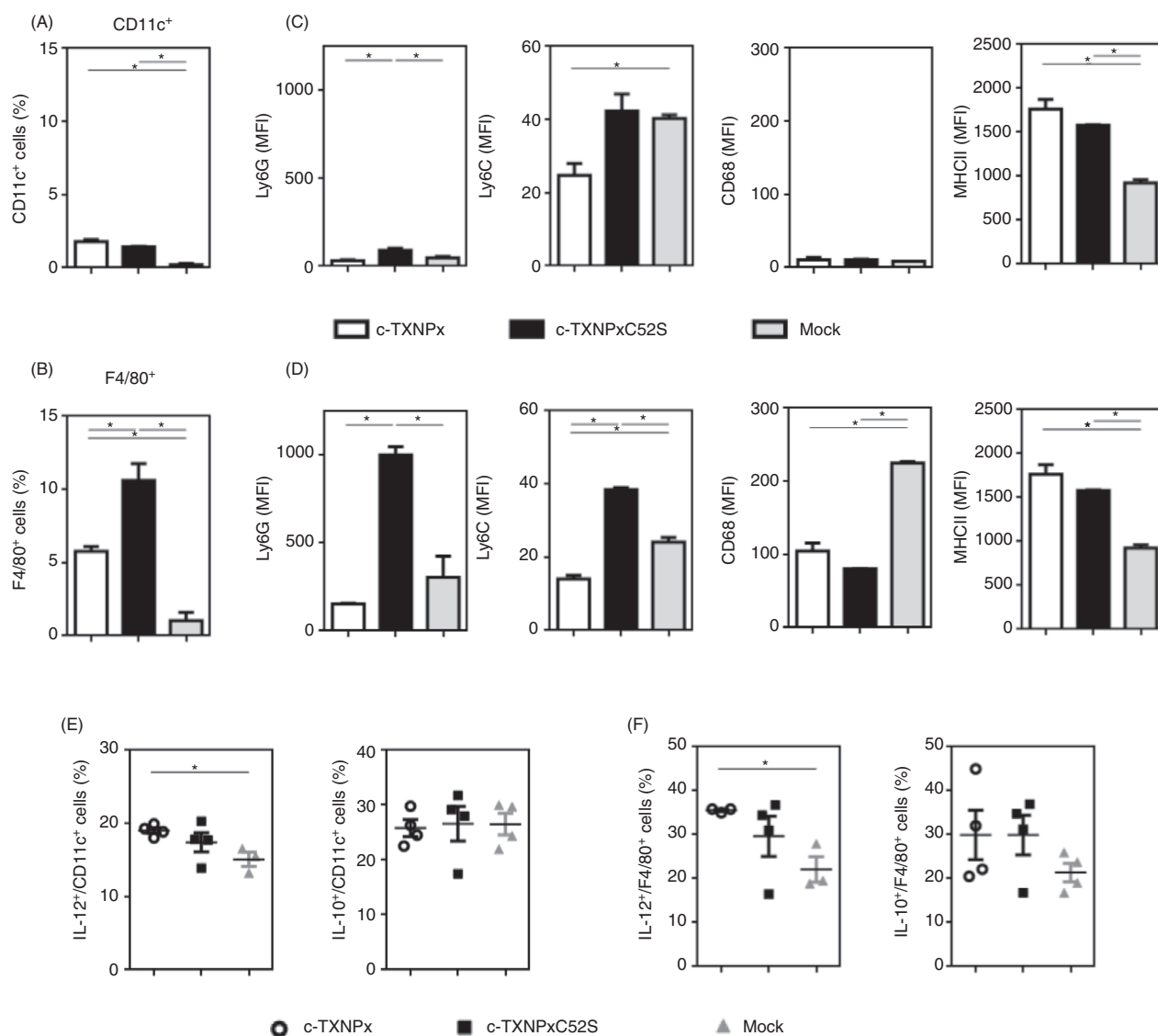


**Figure 2.** c-TXNPx favours the recruitment of IL-12/23p40-producing F4/80<sup>+</sup> and CD11<sup>+</sup> cells to the peritoneal cavity. Mice were i.p. injected with c-TXNPx or c-TXNPxC52S in PBS 6 times every two days. Then, PECs were removed and analysed by flow cytometry. Percentage of CD11c<sup>+</sup> F4/80<sup>-</sup> cells (A) and F4/80<sup>+</sup> CD11c<sup>-</sup> cells (B) in PEC. Surface expression of Ly6C, Ly6G, MHC class II and CD68 was examined in CD11c<sup>+</sup> F4/80<sup>-</sup> (C) or F4/80<sup>+</sup> CD11c<sup>-</sup> (D)-gated cells. Data are expressed as mean of fluorescence intensity (MFI)  $\pm$  SEM. Percentage of IL-12/23p40<sup>+</sup> or IL-10<sup>+</sup> cells on CD11c<sup>+</sup> F4/80<sup>-</sup> (E) and F4/80<sup>+</sup> CD11c<sup>-</sup>-gated cells (F). Data are representative of three independent experiments ( $\pm$ SEM, indicated by error bars). Asterisks indicate statistically significant differences (\*P < 0.05).

the control group (Figure 3B). Splenocytes from these mice also secreted high levels of IFN- $\gamma$ , although lower than when stimulated with the wt protein, while no changes were detected for IL-4 (Figure 3B). A similar result was obtained when T cells from mice *in vivo* primed with the mutated trypanedoxin peroxidase were restimulated *in vitro* with c-TXNPx (c-TXNPxC52S/c-TXNPx). However, these cells produced very low levels of IFN- $\gamma$  and IL-4 (Figure 3C), although CD4 T-cell proliferation was detected. These results suggest that active c-TXNPx is necessary to prime IFN- $\gamma$ -producing CD8<sup>+</sup> T

cells while the mutated c-TXNPxC52S is unable to expand c-TXNPxC52S-specific CD8<sup>+</sup> T cells. They also suggest that the main source of IFN- $\gamma$  is likely primed CD8<sup>+</sup> T cells.

Taking into consideration that c-TXNPxC52S induced an impaired T-cell response, we wondered whether this weak cellular response also affected antibody production. With this aim, we analysed the antibody titre for c-TXNPx-specific IgG, IgM and IgG2a from sera of c-TXNPx- or c-TXNPxC52S-injected mice. As shown in Figure 4, although both groups injected with trypanedoxin

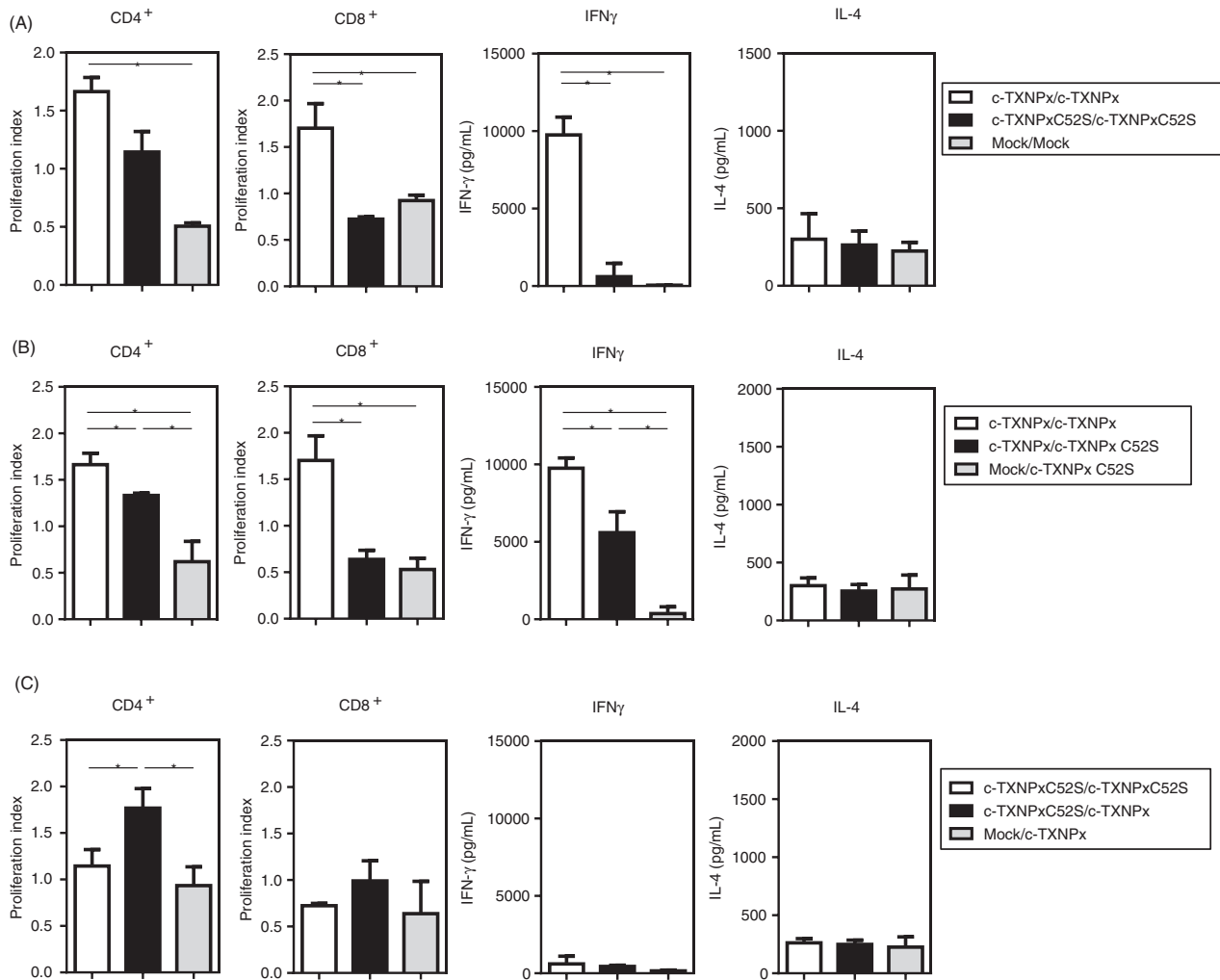


**Figure 3.** c-TXNPx induces CD4<sup>+</sup> and CD8<sup>+</sup> T-cell proliferation with IFN- $\gamma$  production. T-cell proliferation and cytokine production by splenocytes from wt and mutated c-TXNPx-treated mice. Mice were i.p. injected with c-TXNPx, c-TXNPxC52S or mock (control) in PBS 6 times every two days. Spleens were removed, labelled with CFSE and cultured in the presence of different stimuli, to evaluate CD4 and CD8 T-cell proliferation and cytokine production in culture supernatants by specific ELISA. (A) Splenocytes primed with c-TXNPx or c-TXNPxC52S and *in vitro* stimulated with the corresponding immunogens, c-TXNPx (c-TXNPx/c-TXNPx) or c-TXNPxC52S (c-TXNPx/c-TXNPxC52S). (B) Splenocytes primed with c-TXNPx and *in vitro* stimulated with c-TXNPx (c-TXNPx/c-TXNPx) or c-TXNPxC52S (c-TXNPx/c-TXNPxC52S). (C) Splenocytes primed with c-TXNPxC52S and *in vitro* stimulated with c-TXNPx (c-TXNPxC52S/c-TXNPx) or c-TXNPxC52S (c-TXNPxC52S/c-TXNPxC52S). Controls consisted in *in vivo* priming with mock preparation. The proliferation index was calculated with respect to cells incubated in the presence of medium alone on CD4 or CD8-gated cells. IFN- $\gamma$  and IL-4 were determined on culture supernatants by ELISA. Data shown are the mean of three independent experiments  $\pm$  SEM,  $n = 6$  animals per group. Asterisks indicate statistically significant differences ( $*P < 0.05$ ).

peroxidases presented high levels of IgG and IgG2a, no differences were detected between the groups injected with either c-TXNPx or c-TXNPxC52S, suggesting that the antibody response was not affected by the replacement of Cys 52 for a Ser.

#### The C<sub>p</sub> is necessary for IFN- $\gamma$ production by T cells during natural *T. cruzi* infection

In order to study the immune response triggered during the infection, we analysed the cellular and humoral

immune response developed in the context of parasite natural infection and its association with c-TXNPx enzymatic activity. To this end, sera and PBMC were collected from a cohort of patients with chronic Chagas disease, without demonstrable pathology (G0) and with Chagas cardiomyopathy (G1), as well as non-infected individuals (NI) as control group. First, we evaluated the specific proliferative response and IFN- $\gamma$  secretion of PBMC from patients of each group and compared this response with that of PBMC from non-infected individuals. Results showed that c-TXNPx, but not c-TXNPxC52S,

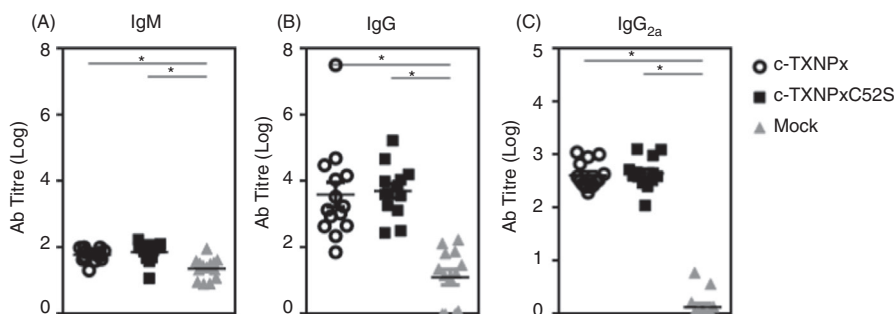


**Figure 4.** Both c-TXNPx and c-TXNPxC52S induce specific IgG antibodies. Mice were i.p. injected with c-TXNPx or c-TXNPxC52S in PBS 6 times every two days. c-TXNPx- or c-TXNPxC52S-specific antibodies were detected in sera by ELISA. Data represent the results of three independent experiments. Titres are shown as the mean  $\pm$  SEM of the log<sub>10</sub> titres. Each dot corresponds to the value from a single individual. Asterisks indicate statistically significant differences ( $*P < 0.05$ ).

stimulation induced proliferation compared with mock in G0 and G1 patients but not in NI donors (Figure 5A). Similarly, levels of IFN- $\gamma$  were increased upon stimulation with c-TXNPx compared with mock in G0 and G1 patients but not in non-infected donors, while no significant production of IFN- $\gamma$  was detected when stimulating with c-TXNPxC52S (Figure 5B).

Regarding the proliferation data, although no difference was observed between c-TXNPxC52S and mock in G0 patients, results showed that the effect induced by the mutated protein was higher in patients without demonstrable cardiac involvement compared with NI subjects (Figure 5A).

Finally, to determine the presence of a humoral response specific of c-TXNPx and c-TXNPxC52S we measured total specific IgG in sera from G0 and G1 patients, and NI individuals by ELISA. IgG antibodies from patients without demonstrable cardiac manifestations (G0) and NI controls better recognized c-TXNPx than c-TXNPxC52S (Figure 5C).

## Discussion

Prxs are key players during infections and can influence the interplay between parasites and host cells in many ways. Previous work from our group and others showed that *T. cruzi* cytosolic Prx c-TXNPx is a virulence factor, released by the different life stages of the parasite.<sup>21,22</sup> The main objective of this work was to understand the interaction between c-TXNPx and the immune system and to analyse the role of the redox active cysteine C<sub>p</sub> on its immunological properties.

The biochemical and functional characterization of recombinant c-TXNPx and c-TXNPxC52S showed that both proteins, although having a single amino acid change (Cys by Ser), exhibit structural and functional differences. As expected, the mutation of the C<sub>p</sub> abolished the peroxidase activity as c-TXNPx depends on both C<sub>p</sub> and C<sub>R</sub> for its enzymatic activity, as well as the presence

of a regenerating system.<sup>31</sup> Furthermore, they also differed slightly in their oligomerization state: c-TXNPx formed an oligomer larger than the decamer and HMM aggregates, whereas c-TXNPxC52S formed a decameric structure together with HMM aggregates as was already shown for non-endotoxin-free proteins and for mitochondrial C<sub>p</sub> mutant m-TXNPxC81S.<sup>39</sup> Prxs from diverse organisms suffer conformational changes, varying from dimers to decamers and HMM aggregates, sensitive to different conditions such as redox state, among others<sup>40</sup>; that is the case of wild-type and its inactive version, which modify their oligomerization profile under different oxidation conditions. Moreover, overoxidation of C<sub>p</sub> is associated with inactivation of the peroxidase activity.<sup>15</sup> In our work, the oligomerization profile and the overoxidation studies strongly suggest that the majority of recombinant purified wt c-TXNPx was in the oxidation state, where the C<sub>p</sub> was disulphide bond with the C<sub>R</sub> and could display its peroxidase activity if being regenerated. In spite of this fact, we cannot rule out the possibility that c-TXNPx can be overoxidized and inactivated during the interaction with immune cells. In addition, other factors such as pH and divalent cations also affect oligomerization, as observed in mitochondrial TXNPx from *Leishmania brasiliensis*.<sup>41</sup>

In our murine experimental model, the i.p. injection of both the c-TXNPx and c-TXNPxC52S proteins induced the recruitment of MHCII<sup>+</sup> CD11c<sup>+</sup> F4/80<sup>-</sup> and MHCII<sup>+</sup> CD11c<sup>-</sup> F4/80<sup>+</sup> cells in the peritoneum, which could account for activated dendritic cells and macrophages, respectively. However, both the frequency of macrophages and their Ly6G expression were increased in c-TXNPxC52S-injected animals indicating that the characteristics and/or the dynamics of the immune response differ in the absence or presence of redox active C<sub>p</sub> of c-TXNPx. Furthermore, only wild-type c-TXNPx induced a statistically significant increase in IL-12/23p40 expression by both dendritic cells and macrophages, indicating that C<sub>p</sub> is necessary for triggering the production of this

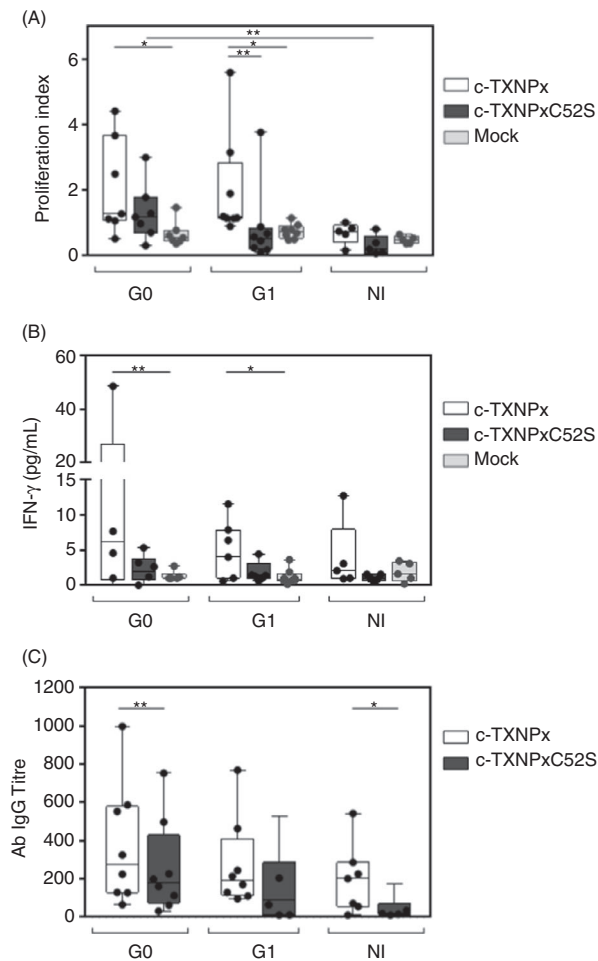


**Figure 5.** Cellular and humoral immune response from chronic Chagas disease patients triggered by c-TXNPx and c-TXNPxC52S. PBMC from chronic Chagas patients without demonstrable cardiac involvement (G0,  $n = 7$ ), with Chagas cardiomyopathy (G1,  $n = 8$ ), and non-infected donors (NI,  $n = 5$ ) were incubated with recombinant c-TXNPx or c-TXNPxC52S, mock and no antigen (culture medium only as controls) for 5 days in complete RPMI medium. Each condition was performed by triplicate. (A) Cells were pulsed with  $^3\text{H}$ -thymidine for the last 18 h of incubation, and PBMC proliferation was determined by  $^3\text{H}$ -thymidine uptake. (B) Culture supernatants were collected after 5 days of stimulation with c-TXNPx, c-TXNPxC52S or mock, and IFN- $\gamma$  secretion was quantified by ELISA. Box-and-whisker plots (min to max) show the stimulation index (SI) that was calculated for each readout as the mean value for triplicate stimulated cultures of each individual divided by the mean value of triplicate non-stimulated cultures (medium only). In cases for which the level of secreted IFN- $\gamma$  was undetectable, the obtained value from the stimulated cultures was divided by the lowest detectable value (2.3 pg/ml). (C) Anti-c-TXNPx (dots) and anti-c-TXNPxC52S (squares) antibody titration was carried out in sera from chronic Chagas disease patients without demonstrable cardiac manifestations (G0,  $n = 8$ ) and with Chagas cardiomyopathy (G1,  $n = 8$ ), and non-infected donors (NI,  $n = 7$ ) by ELISA. The titre of antibodies from each individual was expressed as the serum dilution factor that corresponds to the IC<sub>50</sub> value of the adjusted curve, which was calculated by non-linear regression analysis. Each dot corresponds to the value from a single individual, and the horizontal line shows the median value for each group. Statistical analysis was performed using a linear mixed-effects model (LMM) fitted by maximum likelihood and Tukey's honest significant difference contrasts for post hoc comparisons. Asterisks indicate statistically significant differences (\*\*\* $P < 0.001$ ; \*\* $P < 0.01$ ; \* $P < 0.05$ ).

inflammatory cytokine. The distinct modulatory properties of c-TXNPx and c-TXNPxC52S were also confirmed *in vitro* on macrophages in our laboratory (data not shown).

Our results are in line with previous reports about the inflammatory properties of Prxs. Indeed, human Prx1, Prx2 and Prx4 can induce the secretion of IL-6 and TNF- $\alpha$  by murine macrophages.<sup>42</sup> In addition, some Prxs can trigger a TLR4/TLR2/NF- $\kappa$ B-mediated pro-inflammatory immune response.<sup>43</sup> In this sense, human Prx1 stimulates the secretion of pro-inflammatory cytokines by human macrophages through TLR4 receptor in a process that does not depend on its peroxidase activity but on both its chaperone activity and its ability to form decamers, indicating the importance of quaternary structure in this process.<sup>44</sup> Our results suggest that structural differences in quaternary structures of c-TXNPx and c-TXNPxC52S could account on the observed differences in the induction of pro-inflammatory responses. Structural differences could influence not only antigen processing by dendritic cells or macrophages but also their recognition by a given receptor. In fact, different endocytic pathways have been

described depending on the size and characteristics of an antigen.<sup>45</sup> However, we cannot rule out the possibility that the peroxidase activity is also participating in this process.

Apart from the enzymatic and structural differences between c-TXNPx and c-TXNPxC52S, the presence or absence of C<sub>p</sub> could also impact on cell signalling; it is well established that reversible oxidation of redox sensitive proteins by Prxs modulates the function of transcription factors, kinases and phosphatases.<sup>46,47</sup> This reversible oxidation state of proteins mediated by Prxs is independent on the regenerating system but dependent on C<sub>p</sub>.<sup>48</sup> Indeed, Prx2 and H<sub>2</sub>O<sub>2</sub> mediate the inactivation of the transcription factor STAT3 and some cytokines.<sup>49</sup> Furthermore, human Prx1 and Prx2, first oxidized by H<sub>2</sub>O<sub>2</sub>, transfer their disulphide oxidation state to the nuclear protein HMGB1, enabling its secretion by monocytes/macrophages in response to inflammatory stimuli.<sup>50</sup> In the light of these findings, we can speculate that the transfer of disulphide oxidation by wt c-TXNPx to cellular targets could mediate the observed pro-inflammatory response.

Prxs from different parasites also have particular immunomodulatory properties. Helminth Prx induces the alternative activation of macrophages by inducing the production of IL-4, IL-5 and IL-13 and the polarization of T cells towards a Th2 immune response, that is independent on peroxidase activity and dependent on the structure.<sup>26</sup> However, the Prx from *T. gondii* can mediate both the induction of alternative activated macrophages in an *in vitro* murine model,<sup>28</sup> and inflammatory macrophages together with a Th1 response in mice.<sup>51</sup> This discrepancy highlights the complexity of the interaction between Prxs and immune cells. Our results clearly show that c-TXNPx from the protozoan *T. cruzi* induces a pro-inflammatory phenotype and a Th1 response. Similar results were also obtained with a Prx from *P. berghei*, as it promotes a pro-inflammatory immune response characterized by the induction of IL-12/23p40 and TNF- $\alpha$ .<sup>25</sup>

In agreement with the induction of IL-12/23p40 production by macrophages and dendritic cells, the wt c-TXNPx, but not the mutant, promoted specific CD4<sup>+</sup> and CD8<sup>+</sup> T-cell proliferation with high production of IFN- $\gamma$ , indicating that the C<sub>P</sub> is involved in the Th1 polarization. It is possible that the activation of innate immune cells is impaired in animals stimulated with c-TXNPxC52S due to structural or functional properties of the protein, affecting the adaptive immune response. For instance, we could postulate that dendritic cells cannot cross-present c-TXNPxC52S as efficiently as c-TXNPx, affecting the CD8<sup>+</sup> T-cell activation. Interestingly, as c-TXNPx, the Prx-1 from *T. gondii* induces a specific Th1 response with IFN- $\gamma$  production.<sup>51</sup> The fact that c-TXNPxC52S-primed CD4<sup>+</sup> T cells were not able to produce IFN- $\gamma$  when restimulated with either the mutant or wt enzyme suggests that cells could be anergic or unresponsive. Anergic or hyporesponsive T cells lose the proliferative capacity and express anergic molecules, such as GRAIL, Otubain-1, CTLA-4 and PD-1.<sup>52</sup> Interestingly, *T. cruzi*-infected mice present an impaired T-cell response characterized by low IL-2 and IFN- $\gamma$  secretion.<sup>53</sup> Thus, *T. cruzi* might control T-cell proliferation or responsiveness according to the secretion of specific molecules, depending on the phase of the infection. Our results suggest that c-TXNPx could be involved in the immune response induced upon *T. cruzi* infection, as this protein, such as others, induces dendritic cell maturation and specific IFN- $\gamma$ -producing Th1 cells.<sup>22,54–57</sup> Moreover, these data were confirmed in the context of natural infections as c-TXNPx, but not its inactive form, induced PBMC proliferation and IFN- $\gamma$  secretion. However, as described previously,<sup>30</sup> only a faint immune response is observed in patients without clinical alterations, which may constitute a mechanism to protect this relevant enzyme from the immune attack.

Despite the fact that c-TXNPxC52S induced an impaired T-cell response, the mutant was capable of

inducing comparable levels of specific antibodies than c-TXNPx, suggesting that conformational epitopes are not modified, while antigen presentation in the context of MHC class II could be compromised. As there are IgG antibodies against c-TXNPxC52S, it is evident that there was a collaboration of T cells that allowed the class change as the T-cell-independent production of antibodies does not involve this process.<sup>58</sup> Perhaps, the collaboration of CD4 Th1 cells in animals inoculated with c-TXNPxC52S occurred before the helper T cells were hyporesponsive. To evaluate this hypothesis, it would be necessary to analyse the early immune response against the protein. Nevertheless, we detected significant difference in specific antibody against the wt c-TXNPx compared with the mutant C<sub>P</sub> counterpart in patients without demonstrable cardiac manifestations (G0), demonstrating that the c-TXNPx-specific IgG antibodies induced in the context of the infection do not recognize c-TXNPxC52S as efficiently as c-TXNPx, likely due to the complexity of the antigen-presentation process in particular and the immune milieu in general, from which the proteins are presented to B and T cells, which differ from the immunization setting in mice.

In conclusion, we show that c-TXNPx induces the recruitment of IL-12/23p40-producing innate APCs, associated with a strong specific Th1 immune response. Both functional activities depend on the presence of the C<sub>P</sub>, responsible for its peroxidase activity and implicated in its oligomeric conformation. These results are important in the understanding of the immunological response induced by a known virulence factor of *T. cruzi*, and could contribute to the rational design of immune-based strategies against Chagas disease.

## Acknowledgements

We wish to thank the Animal Facilities located at the Facultad de Medicina (UdelaR) and Institut Pasteur de Montevideo and the Cell Biology Unit at the Institut Pasteur de Montevideo. We thank all the patients and non-infected individuals who participated in this study. We are also very grateful to the staff of the Instituto Nacional de Parasitología 'Doctor Mario Fatala Chabén', Buenos Aires, Argentina, Violeta Chiauzzi from Instituto de Biología y Medicina Experimental (IBYME-CONICET) and Sofía Micolini from Instituto de Ingeniería Genética y Biología Molecular 'Prof. Héctor N. Torres' (INGEBI-CONICET) for technical assistance in blood sample collection. We also wish to thank financial supports from Comisión Sectorial de Investigación Científica (CSIC I+D 2015 to María Dolores Piñeyro and Carlos Robello), Universidad de la República, Montevideo, Uruguay, Programa de Desarrollo de Ciencias Básicas (PEDECIBA), Sistema Nacional de Investigadores from the Agencia Nacional de Investigación e Innovación (SNI-ANII), Consejo Nacional



de Investigaciones Científicas y Tecnológicas [CONICET; Grant number 112-200801-02915] and by the Agencia Nacional de Promoción Científica y Tecnológica [ANPCyT; Grant number 2014-1026] to Karina Gómez.

## Conflict of interest

The authors declare no competing financial and commercial interests in relation to the manuscript.

## Data availability statement

Data relating to the manuscript will be available upon reasonable request to the corresponding author.

## References

- WHO. <http://www.WHO.int/mediacentre/factsheets/fs340/en/index.htm>. Accessed 10 March 2020.
- Schmunis GA, Yadon ZE. Chagas disease: a Latin American health problem becoming a world health problem. *Acta Trop*. 2010; **115**(1–2):14–21.
- Perez-Molina JA, Molina I. Chagas disease cardiomyopathy treatment remains a challenge - Authors' reply. *Lancet* 2018; **391**(10136):2209–10.
- Urbina JA. The long road towards a safe and effective treatment of chronic Chagas disease. *Lancet Infect Dis*. 2018; **18**(4):363–5.
- Acevedo GR, Girard MC, Gomez KA. The unsolved jigsaw puzzle of the immune response in Chagas disease. *Front Immunol*. 2018; **9**:1929.
- Tarleton R. Immune system recognition of *Trypanosoma cruzi*. *Curr Opin Immunol*. 2007; **19**(4):430–4.
- Castro H, Tomas AM. Peroxidases of trypanosomatids. *Antioxid Redox Signal*. 2008; **10**(9):1593–606.
- Perkins A, Nelson KJ, Parsonage D, Poole LB, Karplus PA. Peroxiredoxins: guardians against oxidative stress and modulators of peroxide signaling. *Trends Biochem Sci*. 2015; **40**(8):435–45.
- Pineyro MD, Parodi-Talice A, Arcari T, Robello C. Peroxiredoxins from *Trypanosoma cruzi*: virulence factors and drug targets for treatment of Chagas disease? *Gene* 2008; **408**(1–2):45–50.
- Piacenza L, Peluffo G, Alvarez MN, Kelly JM, Wilkinson SR, Radi R. Peroxiredoxins play a major role in protecting *Trypanosoma cruzi* against macrophage- and endogenously-derived peroxynitrite. *Biochem J*. 2008; **410**(2):359–68.
- Zago MP, Hosakote YM, Koo SJ, Dhiman M, Pineyro MD, Parodi-Talice A, et al. TcI isolates of *Trypanosoma cruzi* exploit the antioxidant network for enhanced intracellular survival in macrophages and virulence in mice. *Infect Immun*. 2016; **84**(6):1842–56.
- Veal EA, Underwood ZE, Tomalin LE, Morgan BA, Pillay CS. Hyperoxidation of peroxiredoxins: gain or loss of function? *Antioxid Redox Signal*. 2018; **28**(7):574–90.
- Yang KS, Kang SW, Woo HA, Hwang SC, Chae HZ, Kim K, et al. Inactivation of human peroxiredoxin I during catalysis as the result of the oxidation of the catalytic site cysteine to cysteine-sulfinic acid. *J Biol Chem*. 2002; **277**(41):38029–36.
- Wood ZA, Poole LB, Karplus PA. Peroxiredoxin evolution and the regulation of hydrogen peroxide signaling. *Science* 2003; **300**(5619):650–3.
- Pineyro MD, Arias D, Ricciardi A, Robello C, Parodi-Talice A. Oligomerization dynamics and functionality of *Trypanosoma cruzi* cytosolic trypanredoxin peroxidase as peroxidase and molecular chaperone. *Biochim Biophys Acta*. 2019; **1863**(10):1583–94.
- Ishii TW, Warabi E, Yanagawa T. Novel roles of peroxiredoxins in inflammation, cancer and innate immunity. *J Clin Biochem Nutr*. 2012; **50**(2):91–105.
- Knoops B, Argyropoulou V, Becker S, Ferte L, Kuznetsova O. Multiple roles of peroxiredoxins in inflammation. *Mol Cells*. 2016; **39**(1):60–4.
- Catterall JB, Rowan AD, Sarsfield S, Saklatvala J, Wait R, Cawston TE. Development of a novel 2D proteomics approach for the identification of proteins secreted by primary chondrocytes after stimulation by IL-1 and oncostatin M. *Rheumatology* 2006; **45**(9):1101–9.
- Chang JW, Lee SH, Lu Y, Yoo YJ. Transforming growth factor-beta1 induces the non-classical secretion of peroxiredoxin-I in A549 cells. *Biochem Biophys Res Commun*. 2006; **345**(1):118–23.
- Robinson MW, Menon R, Donnelly SM, Dalton JP, Ranganathan S. An integrated transcriptomics and proteomics analysis of the secretome of the helminth pathogen *Fasciola hepatica*: proteins associated with invasion and infection of the mammalian host. *Mol Cell Proteomics*. 2009; **8**(8):1891–907.
- Bayer-Santos E, Aguilar-Bonavides C, Rodrigues SP, Cordero EM, Marques AF, Varela-Ramirez A, et al. Proteomic analysis of *Trypanosoma cruzi* secretome: characterization of two populations of extracellular vesicles and soluble proteins. *J Proteome Res*. 2013; **12**(2):883–97.
- Gadelha FR, Goncalves CC, Mattos EC, Alves MJ, Pineyro MD, Robello C, et al. Release of the cytosolic trypanredoxin peroxidase into the incubation medium and a different profile of cytosolic and mitochondrial peroxiredoxin expression in H2O2-treated *Trypanosoma cruzi* tissue culture-derived trypomastigotes. *Exp Parasitol*. 2013; **133**(3):287–93.
- Geiger A, Hirtz C, Becue T, Bellard E, Centeno D, Gargani D, et al. Exocytosis and protein secretion in *Trypanosoma*. *BMC Microbiol*. 2010; **10**:20.
- Brossas JY, Gulin JEN, Bisio MMC, Chapelle M, Marinach-Patrice C, Bordessoules M, et al. Secretome analysis of *Trypanosoma cruzi* by proteomics studies. *PLoS One*. 2017; **12**(10):e0185504.
- Furuta T, Imajo-Ohmi S, Fukuda H, Kano S, Miyake K, Watanabe N. Mast cell-mediated immune responses through IgE antibody and Toll-like receptor 4 by malarial peroxiredoxin. *Eur J Immunol*. 2008; **38**(5):1341–50.
- Donnelly S, Stack CM, O'Neill SM, Sayed AA, Williams DL, Dalton JP. Helminth 2-Cys peroxiredoxin drives Th2 responses through a mechanism involving alternatively activated macrophages. *FASEB J*. 2008; **22**(11):4022–32.
- Donnelly S, O'Neill SM, Sekiya M, Mulcahy G, Dalton JP. Thioredoxin peroxidase secreted by *Fasciola hepatica* induces the alternative activation of macrophages. *Infect Immun*. 2005; **73**(1):166–73.
- Marshall ES, Elshekha HM, Hakimi MA, Flynn RJ. Toxoplasma gondii peroxiredoxin promotes altered macrophage function, caspase-1-dependent IL-1beta secretion enhances parasite replication. *Vet Res*. 2011; **42**:80.
- Robinson MWH, Dalton A, Donnelly JP, Donnelly S. Peroxiredoxin: a central player in immune modulation. *Parasite Immunol* 2010; **32**(5):305–13.
- Girard MC, Acevedo GR, Lopez L, Ossowski MS, Pineyro MD, Grosso JP, et al. Evaluation of the immune response against *Trypanosoma cruzi* cytosolic trypanredoxin peroxidase in human natural infection. *Immunology* 2018; **155**(3):367–78.
- Pineyro MD, Arcari T, Robello C, Radi R, Trujillo M. Trypanredoxin peroxidases from *Trypanosoma cruzi*: High efficiency in the catalytic elimination of hydrogen peroxide and peroxynitrite. *Arch Biochem Biophys*. 2011; **507**(2):287–95.
- Planesse C, Nativel B, Iwema T, Gasque P, Robert-Da Silva C, Viranaicken W. Recombinant human HSP60 produced in *ClearColi BL21(DE3)* does not activate the NF-kappaB pathway. *Cytokine*. 2015; **73**(1):190–5.
- Malyala P, Singh M. Endotoxin limits in formulations for preclinical research. *J Pharm Sci*. 2008; **97**(6):2041–4.
- Ribeiro AL, Nunes MP, Teixeira MM, Rocha MO. Diagnosis and management of Chagas disease and cardiomyopathy. *Nat Rev Cardiol*. 2012; **9**(10):576–89.
- Hothorn T, Bretz F, Westfall P. Simultaneous inference in general parametric models. *Biomet J Biomet Zeitsch*. 2008; **50**(3):346–63.
- Angelucci F, Miele AE, Ardini M, Boumis G, Saccoccia F, Bellelli A. Typical 2-Cys peroxiredoxins in human parasites: Several physiological roles for a potential chemotherapy target. *Mol Biochem Parasitol*. 2016; **206**(1–2):2–12.
- Jang HH, Lee KO, Chi YH, Jung BG, Park SK, Park JH, et al. Two enzymes in one; two yeast peroxiredoxins display oxidative stress-dependent switching from a peroxidase to a molecular chaperone function. *Cell*. 2004; **117**(5):625–35.
- DiPiazza AT, Hill JP, Graham BS, Ruckwardt TJ. OMIP-061: 20-color flow cytometry panel for high-dimensional characterization of murine antigen-presenting cells. *Cytometry*. 2019; **95**(12):1226–30.
- Teixeira F, Castro H, Cruz T, Tse E, Koldewey P, Southworth DR, et al. Mitochondrial peroxiredoxin functions as crucial chaperone reservoir in *Leishmania infantum*. *Proc Natl Acad Sci USA* 2015; **112**(7):E616–24.
- Barranco-Medina S, Lazaro JJ, Dietz KJ. The oligomeric conformation of peroxiredoxins links redox state to function. *FEBS Lett*. 2009; **583**(12):1809–16.
- Morais MA, Giuseppe PO, Souza TA, Alegria TG, Oliveira MA, Netto LE, et al. How pH modulates the dimer-decamer interconversion of 2-Cys peroxiredoxins from the Prx1 subfamily. *J Biol Chem*. 2015; **290**(13):8582–90.
- Zhao LX, Du JR, Zhou HJ, Liu DL, Gu MX, Long FY. Differences in proinflammatory property of six subtypes of peroxiredoxins and anti-inflammatory effect of ligustilide in macrophages. *PLoS One*. 2016; **11**(10):e0164586.
- Shichita T, Hasegawa E, Kimura A, Morita R, Sakaguchi R, Takada I, et al. Peroxiredoxin family proteins are key initiators of post-ischemic inflammation in the brain. *Nat Med*. 2012; **18**(6):911.
- Riddell JR, Wang X-Y, Minderman H, Gollnick SO. Peroxiredoxin 1 stimulates secretion of proinflammatory cytokines by binding to TLR4. *J Immunol*. 2010; **184**(2):1022–30.

- 45 Xiang SD, Scholzen A, Minigo G, David C, Apostolopoulos V, Mottram PL, *et al.* Pathogen recognition and development of particulate vaccines: does size matter? *Methods* 2006; **40**(1):1–9.
- 46 Jonuleit H, Schmitt E, Schuler G, Knop J, Enk AH. Induction of interleukin 10-producing, nonproliferating CD4(+) T cells with regulatory properties by repetitive stimulation with allogeneic immature human dendritic cells. *J Exp Med*. 2000; **192**(9):1213–22.
- 47 Sobotta MC, Liou W, Stocker S, Talwar D, Oehler M, Ruppert T, *et al.* Peroxiredoxin-2 and STAT3 form a redox relay for H<sub>2</sub>O<sub>2</sub> signaling. *Nat Chem Biol*. 2015; **11**(1):64–70.
- 48 Stocker S, Maurer M, Ruppert T, Dick TP. A role for 2-Cys peroxiredoxins in facilitating cytosolic protein thiol oxidation. *Nat Chem Biol*. 2018; **14**(2):148–55.
- 49 Sobotta MC, Liou W, Stöcker S, Talwar D, Oehler M, Ruppert T, *et al.* Peroxiredoxin-2 and STAT3 form a redox relay for H<sub>2</sub>O<sub>2</sub> signaling. *Nat Chem Biol*. 2015; **11**(1):64.
- 50 Kwak MS, Kim HS, Lkhamsuren K, Kim YH, Han MG, Shin JM, *et al.* Peroxiredoxin-mediated disulfide bond formation is required for nucleocytoplasmic translocation and secretion of HMGB1 in response to inflammatory stimuli. *Redox Biol*. 2019; **24**:101203.
- 51 Fereig RM, Kuroda Y, Terkawi MA, Mahmoud ME, Nishikawa Y. Immunization with *Toxoplasma gondii* peroxiredoxin 1 induces protective immunity against toxoplasmosis in mice. *PLoS One* 2017; **12**(4):e0176324.
- 52 Chappert P, Schwartz RH. Induction of T cell anergy: integration of environmental cues and infectious tolerance. *Curr Opin Immunol*. 2010; **22**(5):552–9.
- 53 Stempin CC, Rojas Marquez JD, Ana Y, Cerban FM. GRAIL and Otubain-1 are related to T cell hyporesponsiveness during *Trypanosoma cruzi* Infection. *PLoS Negl Trop Dis*. 2017; **11**(1):e0005307.
- 54 Bivona AE, Sanchez Alberti A, Matos MN, Cerny N, Cardoso AC, Morales C, *et al.* *Trypanosoma cruzi* 80 kDa prolyl oligopeptidase (Tc80) as a novel immunogen for Chagas disease vaccine. *PLoS Negl Trop Dis*. 2018; **12**(3):e0006384.
- 55 Matos MN, Sanchez Alberti A, Morales C, Cazorla SI, Malchiodi EL. A prime-boost immunization with Tc52 N-terminal domain DNA and the recombinant protein expressed in *Pichia pastoris* protects against *Trypanosoma cruzi* infection. *Vaccine* 2016; **34**(28):3243–51.
- 56 Seid CA, Jones KM, Pollet J, Keegan B, Hudspeth E, Hammond M, *et al.* Cysteine mutagenesis improves the production without abrogating antigenicity of a recombinant protein vaccine candidate for human Chagas disease. *Human Vacc Immunotherapeut*. 2017; **13**(3):621–33.
- 57 Chiribao ML, Libisch G, Parodi-Talice A, Robello C. Early *Trypanosoma cruzi* infection reprograms human epithelial cells. *Biomed Res Int*. 2014; **2014**:439501.
- 58 Roco JA, Mesin L, Binder SC, Nefzger C, Gonzalez-Figueroa P, Canete PF, *et al.* Class-switch recombination occurs infrequently in germinal centers. *Immunity* 2019; **51**(2):337–50.e7.

## Supporting Information

Additional Supporting Information may be found in the online version of this article:

**Figure S1.** (A) Study of overoxidation state of recombinant c-TXNPx by western blot. A total of 4 µg of c-TXNPx obtained after endotoxin removal (c-TXNPx P) and overoxidized c-TXNPx treated with 10 mM DTT and 10 mM H<sub>2</sub>O<sub>2</sub> (overox c-TXNPx) were resolved in 12% SDS-PAGE, transferred to nitrocellulose membranes and incubated with anti-SO<sub>2</sub>H or anti-c-TXNPx antibodies. Both samples were analysed in presence (+) or absence (–) of DTT. (B) Oligomerization profiles of c-TXNPx and c-TXNPxC52S resolved on a Superdex 200 10/300. The elution volume of standard proteins was as follows: Thyroglobulin (669 kDa) 9.3 ml; Ferritin (440 kDa) 9.9 ml; Aldolase (158 kDa) 12.6 ml; Ovalbumin (75 kDa) 14.17 ml.

**Figure S2.** Gating strategy for flow cytometry analyses depicted on Figure 2. (A) Gates used to analyse the percentage of F4/80<sup>+</sup> and CD11c<sup>+</sup> cells. (B) Gates used to analyse the percentage of IL-12/23p40<sup>+</sup> or IL-10<sup>+</sup> cells on F4/80<sup>+</sup> and CD11c<sup>+</sup>-gated cells.

**Figure S3.** Gating strategy to analyse the proliferation index of CFSE-labelled splenocytes, shown in Figure 3. The proliferation index was calculated as the ratio between the percentages of CFSE<sup>low</sup> cells in treated and control cells with respect to the control (medium alone).